Effect of Annealing Temperature on The physical Properties of Mn₃O₄ Thin Film Prepared by Chemical Bath Deposition

Cemal Ulutas[1,], Ozge Erken[2], Mustafa Gunes[3], Cebrail Gumus[4]*

[1]Faculty of Education, Hakkari University, 30000 Hakkari, Turkey
[2]Department of Physics, Faculty Science and Letters, Adiyaman University, 02040 Adiyaman, Turkey
[3]Department of Materials Engineering, Engineering and Natural Sciences Faculty, Adana Science and Technology University, 01180 Adana, Turkey
[4]Physics Department, University of Cukurova, 01330 Adana, Turkey
[*]E-mail: cemalulutas@hakkari.edu.tr

In this study, Mn_3O_4 thin film was prepared by the chemical bath deposition (CBD) method on commercial microscope glass substrate deposited at 30 °C. The Mn_3O_4 film was annealed in an air atmosphere for an hour at temperatures 100 °C, 200 °C, 300 °C, 400 °C, 500 °C, respectively. The effect of annealing temperature on structural and optical properties such as optical constants of extinction coefficient (k), refractive index (n), the real (ε_1) and imaginary (ε_2) part of the dielectric constant and energy band gap (E_g) of the film were determined. The experimental characterization techniques included X-ray diffraction (XRD), UV-vis spectrophotometer and Hall effect measurement. XRD analysis showed that the film is grown in a polycrystalline structure in tetragonal phase. The conductivity of the film as a function of annealing temperature was measured as $(1.32\text{-}6.65)\text{x}10^{-6}$ $(\varOmega\text{cm})^{-1}$.

Keywords: Mn_3O_4 film, Chemical bath deposition, Annealing effect, Physical properties

1. INTRODUCTION

Manganese oxide usually exists in three different oxide case (Mn^{2+}, Mn^{3+} and Mn^{4+}) and, naturally are formed in MnO, Mn_2O_3, Mn_3O_4, and MnO_2 form. The magnetic and transport properties of these materials are closely related to their structures, crystal quality and chemical stoichiometry [1]. Mn_3O_4 (space group I4₁/*amd*) lattice parameters $a=b=5.76$ *Å* and $c=9.44$ *Å* oriented along the *c* axis of the tetragonal structure is known as crystallized in a normal spinel structure. Hausmannite Mn_3O_4 ions settle at the tetrahedral A-site as Mn^{2+} cations and in the octahedral B-region as Mn^{3+} cations

consistent with the normal spinal structure [2]. Hausmannite Mn_3O_4 is the most stable manganese oxide and has many important applications such as electrochemical materials [3], electrical storage device [4], humidity sensors [5], rechargeable lithium-ion batteries [6], super capacitor [7,8]. Mn_3O_4 can be obtained with methods such as hydrothermal [9], atomic layer deposition [10], molecular beam epitaxy (MBE) [11,12], electrodeposition [13], metal organic chemical vapor deposition MOCVD [14], calcination [15,16], sol-gel [17], pulsed laser deposition [18], silar method [19] and chemical bath deposition [20]. The most favorable method to grow Mn_3O_4 film is chemical bath deposition compared the other methods due to having number of advantages such as easy preparation, low cost, flexibility to obtained required size, adjustable film thickness depending on the pH, temperature and concentration of the solution.

Although there have been intense research activities on the physical properties of the Mn_3O_4 thin film, very limited studies have been conducted on the effect of annealing temperature on structural and optical properties of the film. In this study, the structural and optical properties of Mn_3O_4 thin film which was prepared by chemical bath deposition were determined taking into account the annealing process in the air atmosphere.
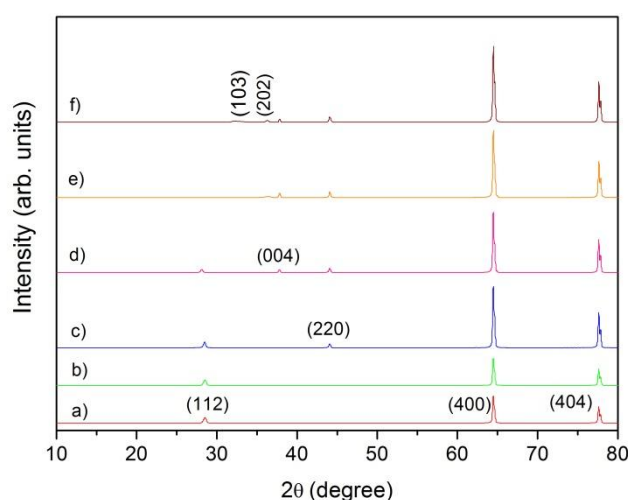

2. EXPERIMENTAL SECTION

Mn_3O_4 thin film was deposited on commercial microscope glass substrate (75 mm x 25 mm x 1 mm in size). Since the quality of the formed film is directly associated with cleaning of the substrates, the glass substrates were cleaned by applying following steps; washed with hot soapy water and rinsed with distilled water and then washed with dilute chromic acid and rinsed in distilled water again. Then after keeping about 3 minutes in propanol passed back to pure water and dried in oven at 100 $^{\circ}$C. To obtain Mn_3O_4 thin film 1 M manganese acetate [$Mn(CH_3COO)_2$] was prepared. To this solution, the buffer solution consisting of ammonia, ammonium chloride (NH_3/NH_4Cl) (pH=10.6) were added. The total pH is found to be 9. The prepared reaction solution was placed in a suitable clean large beaker and stirred with magnetic stirrer until homogeneous and was poured into 20 ml beakers. Cleaned glass substrates were immersed into the beakers in perpendicular. Thus, the deterioration of the film quality by an irregular particle deposition on the film was avoided. 20 ml beaker was placed into 30 $^{\circ}$C oven and adjusted 24 h for each immersion time. The new solution was prepared after each dipping again in order to obtain sufficient film thickness. The dipping was repeated 2 times consecutively. At the end of this period, it occurs that the film formed on glass substrates is composed regular and adheres well to the surface. Optical transmittance of the film at room temperature (%T) and absorbance (A) values were determined using Perkin Elmer UV-vis Lambda-2S spectrophotometer (190-1100 nm), parameters such as conductivity, mobility were determined using Hall measurement system connection (HS-3000 Manual Ver 3.5) and the structural properties by Rigaku RadB X-ray diffractometer with Cu$K_{\alpha1}$ line (λ=1.5405 $\mathring{A}$) in 2θ ranging from 10° to 80° at a speed of 3°/min, with a step size of 0.02°.

3. RESULTS AND DISCUSSION

3.1. Structural properties

Mn_3O_4 thin films were obtained on glass substrates at 30 ^{o}C. This film was successively annealed in air atmosphere in the oven for one hour at temperature range between 100 ^{o}C and 500 ^{o}C. Figure 1(a) shows the XRD pattern of as-deposited Mn_3O_4 film while the others indicates the XRD pattern of annealed films at temperatures 100 °C, 200 ^{o}C, 300 ^{o}C, 400 ^{o}C, 500 ^{o}C, respectively. The diffraction peaks of as-deposited film are obtained as $2\theta=28.50^o$, $2\theta=64.45^o$ and $2\theta=77.59^o$ which corresponds (*112*)*, (400), (404)* planes, respectively. The results showed that the film grew in the tetragonal phase and polycrystalline structure which is in a good agreement with the tetragonal JCPDS card (No:24-0734) of Mn_3O_4.

Figure 1. XRD spectra of Mn_3O_4 thin film annealed at various temperatures for 1 h.a) As-deposited, b) 100 ^{o}C, c) 200 ^{o}C, d) 300 ^{o}C, e) 400 ^{o}C, f) 500 ^{o}C.

As can be seen from the Figure 1(b), there is no significant change in the result of the XRD pattern due to annealing the film at 100 ^{o}C. However, additional peaks are observed at $2\theta=44.07^o$ (*220*) and $2\theta=37.81^o$ (*004*) by annealing the film at 200 ^{o}C and 300 ^{o}C, respectively as shown in Figure 1(c), and Figure 1(d). However, the peak at $2\theta=28.50^o$ (*112*) that obtained at annealing temperature 300 ^{o}C was disappeared at temperature 400 ^{o}C. In the literature, Mn_3O_4 film was transformed into Mn_5O_8 phase as a result of annealing at temperature between 300 ^{o}C and 500 ^{o}C [21,22]. In another report showed that Mn_3O_4 film was reformed in the structure of Mn_2O_3 phase at the same temperature range [23]. However, a mixed structure in Mn_3O_4 and Mn_2O_3 phases were observed in the amorphous form at the annealing temperature range between 250 ^{o}C and 400 ^{o}C and the peak intensity of Mn_3O_4 reduced depending on the annealing temperature and accordingly the peak intensity of Mn_2O_3 phase increased [24]. It can be seen in Figure 1(f) that the diffraction peak intensity of Mn_3O_4 film annealed at 500 ^{o}C increases with annealing temperature without any phase change. This can be explained that the deposited Mn_3O_4 thin film annealed at 500 ^{o}C is more stable than the previous structures in the

reported studies. To better view standard, observed 2θ and d values of Mn_3O_4 thin film are tabulated in Table 1 at investigated annealing temperature range.

Table 1. The effects of annealing temperature on XRD data of Mn_3O_4 thin film.

Annealing Temperature (°C)	Standard Data		Observed Data		FWHM (deg.)	Grain Size (nm)	(hkl)
	2θ (deg.)	d (Å)	2θ (deg.)	d (Å)			
As-deposited	28.88	3.08	28.50	3.12	0.385	21	(112)
	64.65	1.41	64.45	1.44	0.175	53	(400)
	77.51	1.23	77.59	1.22	0.166	60.7	(404)
100	28.88	3.08	28.50	3.12	0.363	22.3	(112)
	64.65	1.41	64.45	1.44	0.166	55.9	(400)
	77.51	1.23	77.59	1.22	0.157	64.2	(404)
200	28.88	3.08	28.48	3.13	0.285	30	(112)
	44.44	2.03	44.03	2.05	0.200	45.4	(220)
	64.65	1.41	64.46	1.44	0.159	61.8	(400)
	77.51	1.23	77.62	1.22	0.167	63.9	(404)
300	28.88	3.08	28.48	3.12	0.260	32.5	(112)
	37.98	2.36	37.81	2.37	0.200	42.9	(004)
	44.44	2.03	44.07	2.05	0.170	53.7	(220)
	64.65	1.41	64.46	1.44	0.153	64.2	(400)
	77.51	1.23	77.60	1.22	0.159	66.9	(404)
400	36.45	2.46	36.40	2.46	0.850	10.3	(202)
	37.98	2.36	37.83	2.37	0.190	45.9	(004)
	44.44	2.03	44.05	2.05	0.129	69.6	(220)
	64.65	1.41	64.47	1.44	0.159	61.6	(400)
	77.51	1.23	77.62	1.22	0.161	66	(404)
500	32.32	2.76	32.03	2.79	1.380	6.3	(103)
	36.45	2.46	36.28	2.47	0.410	21.2	(202)
	37.98	2.36	37.80	2.37	0.170	52.5	(004)
	44.44	2.03	44.03	2.05	0.180	49.6	(220)
	64.65	1.41	64.47	1.44	0.157	62.6	(400)
	77.51	1.23	77.62	1.22	0.155	68.7	(404)

The grain size of the film was calculated using the Scherrer equation as below;

$$D_{hkl} = \frac{0.9\lambda}{\beta\cos\theta} \qquad (1)$$

where, β full width half maximum (*FWHM*) of the peak, λ wavelength of X-ray (λ=1.5405 Å) and θ the Bragg angle. Annealing temperature dependent grain size values are given in Table 1. As can be seen from the table, the grain size value of the most intense peak (*400*) increased with annealing temperature up to 300 °C and decreased in a small amount at annealing temperature of 400 °C and 500 °C .
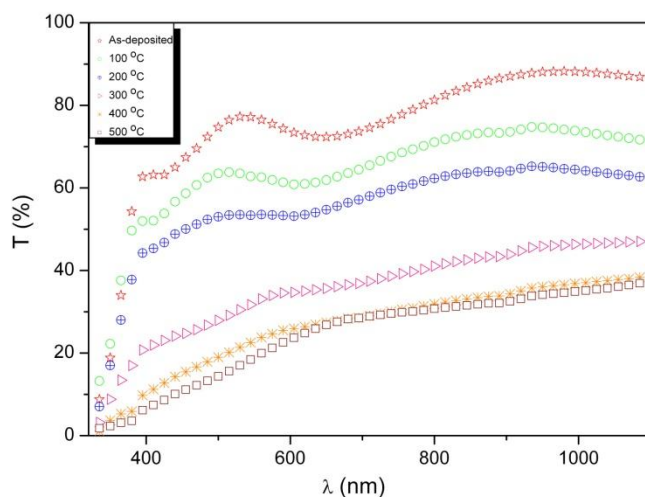
3.2. Electrical properties

Hall effect measurement was performed on annealed Mn_3O_4 thin film that obtained at 30 °C to determine the electrical conductivity (σ) and carrier mobility (μ). Silver paste was used to obtain ohmic contacts on the film. Hall mobility and electrical conductivity are measured as 19-732 $cm^2(Vs)^{-1}$ and $(1.32-6.65)x10^{-6}$ $(\Omega cm)^{-1}$, respectively showing p-type characteristic. Our electrical conductivity results are in a good agreement with the following reference in the literature [25].

3.3. Optical properties

The optical transmittance of annealed and as-deposited Mn_3O_4 thin film was obtained by using UV-vis spectrophotometer at the operational spectral range from 300 nm to 1100 nm at room temperature. Figure 2 shows the optical transmittance of the film as a function of swept wavelength. The average transmittance of as-deposited film at room temperature is about 77 % at wavelength of 550 nm while it is reduced to 63 %, 53 %, 31 %, 23 % and 18 % with annealing temperatures 100 °C, 200 °C, 300 °C, 400 °C and 500 °C, respectively.

It is concluded that the transmittance decreases with increasing annealing temperature in the visible range which is supported by the following reference in the literature [17].
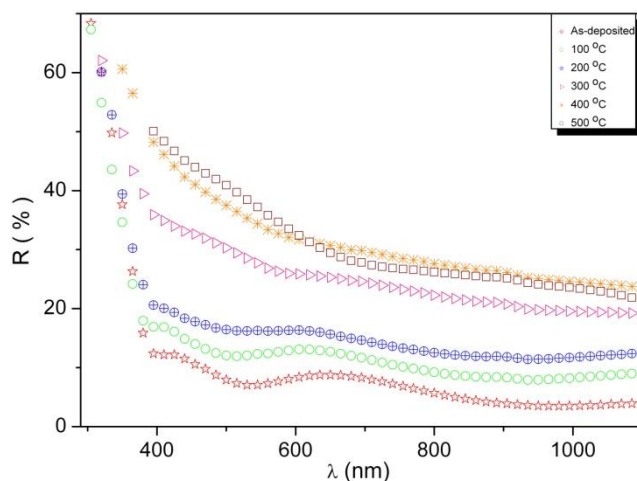

Figure 2. The optical transmittance spectra of Mn_3O_4 thin film as-deposited and annealed in air at 100-500 °C.

We propose that the decrease in the optical transmittance at room temperature was induced by fluid confinement between the grain size on the film. Annealing the film at 100 °C, the liquid on the film evaporates and then causes scattering leaving a less dense environment. This scattering is also observed as absorption in the optical measurement.

Optical transmittance of the thin film is given by the following equation [26] ignoring multiple reflections;

$$T = (1 - R^2)\,exp(-A) \qquad (2)$$

where, R reflection and A absorption, respectively. As seen in Figure 2, optical transmittance at room temperature decreased with increasing annealing temperature while the reflectance increased with increasing annealing temperature as shown in Figure 3.
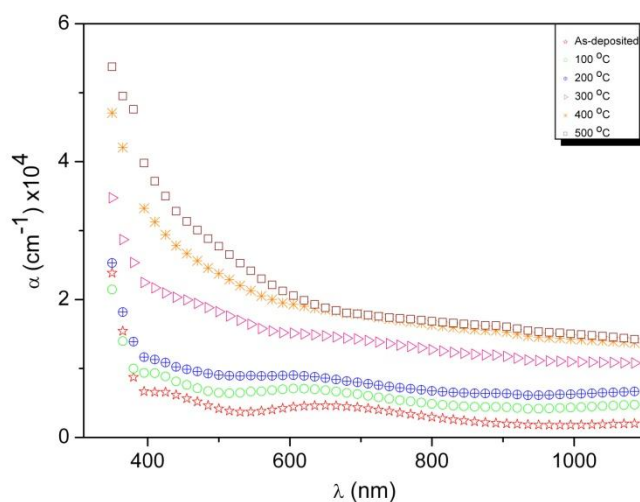

Figure 3. The reflectance spectra of Mn_3O_4 thin film as-deposited and annealed in air at 100-500 ^{o}C.

The absorption coefficient of Mn_3O_4 thin film was calculated using the transmission values by following equation [27].

$$\alpha = -\frac{1}{t}In(T) \tag{3}$$

where, T and t the optical transmittance in the normalized room temperature and film thickness, respectively. Film thickness was calculated as 700 nm using the envelope method [28]. Figure 4 shows wave absorption coefficient as a function of wavelength. As seen in the Figure 4, the absorption coefficient of the film slightly increased at wavelength of 550 nm in the samples annealed at 100 °C and 200 °C. The absorption coefficient value increased with the increase of the annealing temperature.
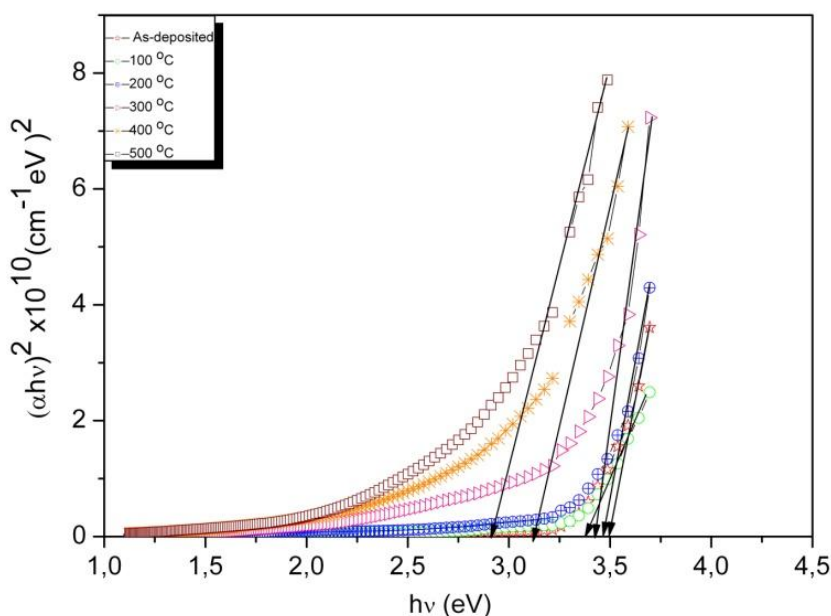

Figure 4. The α versus λ graphs of Mn_3O_4 film as-deposited and annealed in air at 100-500 ^{o}C.

The energy band gap of the film (E_g) was calculated by the following equation.

$$\alpha h v = K\left(h v - E_g\right)^n \tag{4}$$

where α, K, h, v, E_g and n are the absorption coefficient, a constant that depends on transition probability, Planck's constant, the frequency of the photons, optical band gap, and an index that characterizes the optical absorption process, respectively. n gets value of 1/2, 2, 3/2 or 3 for allowed direct, allowed indirect, forbidden direct and forbidden indirect transitions, respectively. In this study, the allowed direct band gaps Mn_3O_4 thin film deposited at various annealing temperatures were determined by plotting $(\alpha h v)^2$ vs. $h v$ curves with the extrapolation of the linear region to low energies as shown in Figure 5. The allowed direct band gap of as-deposited the Mn_3O_4 thin film is 3.55 eV while annealed Mn_3O_4 thin film, the allowed direct band gap 3.38 eV, 3.46 eV, 3.42 eV, 3.12 eV and 2.91 eV at temperatures 100 °C, 200 °C, 300 °C, 400 °C, 500 °C, respectively. As a result of annealing, the energy band gap decreased from 3.55 eV to 2.91 eV. Our finding in energy band gap were found slightly higher than those in the following references which are 2.86 eV [29] and 2.51 eV [20]. However, they are in a good agreement with literature as given 3.28-3.75 eV [30]. This change in band energy is explained in terms of quantum confinement effect [31].
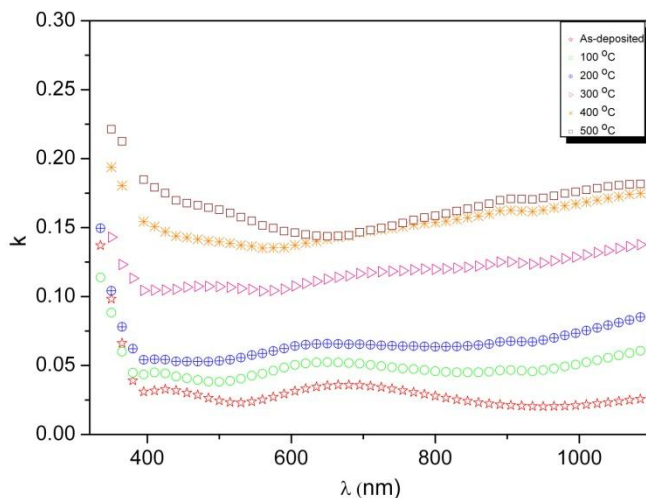

Figure 5. The $(\alpha h v)^2$ versus hv graphs of the Mn_3O_4 film as-deposited and annealed in air at 100-500 °C.

The relationship between the extinction coefficient (*k*) and absorption coefficient (α) is given as [32];

$$k = \frac{\alpha \lambda}{4\pi} \tag{5}$$

where, λ is the wavelength of light. Figure 6 shows the extinction coefficient (*k*) as a function of wavelength. The extinction coefficient of the film varies between 0.024-0.154 range at λ=550 nm.
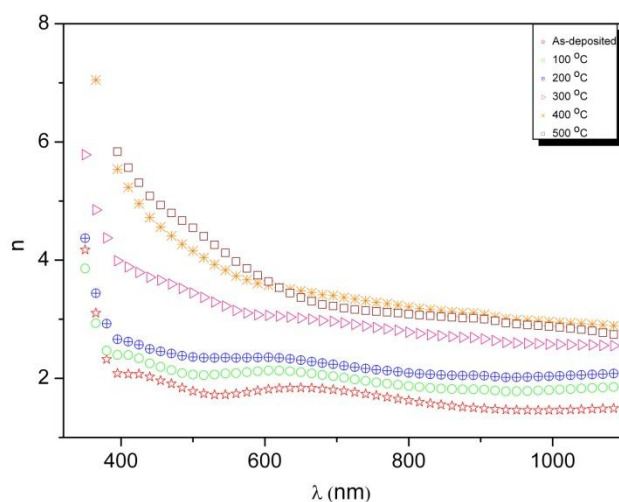
Figure 6. λ dependence of k for Mn_3O_4 film by changes of annealed in air at 100-500 ^{o}C.

The refractive index (*n*) was calculated using the following equation (6) including the reflection and extinction coefficient [33]:

$$n = \frac{1+R}{1-R} + \sqrt{\frac{4R}{(1+R)^2} - k^2}$$

(6)

the refractive index as a function of wavelength is given in Figure 7. The average refractive index was calculated depending on the annealing temperature in the visible region (400-700 nm). However, the refractive index of as-deposited film is found to be 1.79 and increased with increasing annealing temperature. The refractive indexs are 2.09, 2.33, 3.16, 3.72 and 3.84 at temperatures 100 °C, 200 ^{o}C, 300 ^{o}C, 400 ^{o}C and 500 ^{o}C, respectively. The increase in the refractive index can be explained in terms of evaporation of the liquid confinement between the grain sizes with the annealing temperature and remains in place after as the location of the breakers.

Figure 7. The variation of refractive index (n) with wavelength as a function of annealed in air at 100-500 ^{o}C.
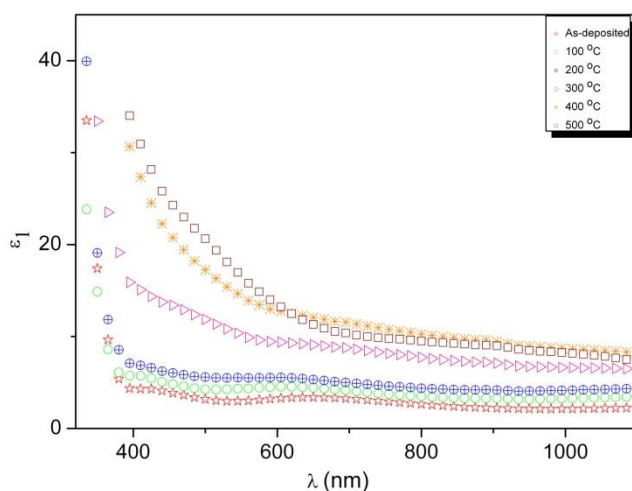
The complex dielectric constant consists of ε_1 and ε_2 where ε_1 indicates the stored energy of the dielectric constant while ε_2 the imaginary part of the dielectric constant corresponding the energy loss in the environment [34]. The real (ε_1) and imaginary (ε_2) parts of the dielectric constant were calculated by equation (7) and (8) depending on refractive index and extinction coefficient [35].
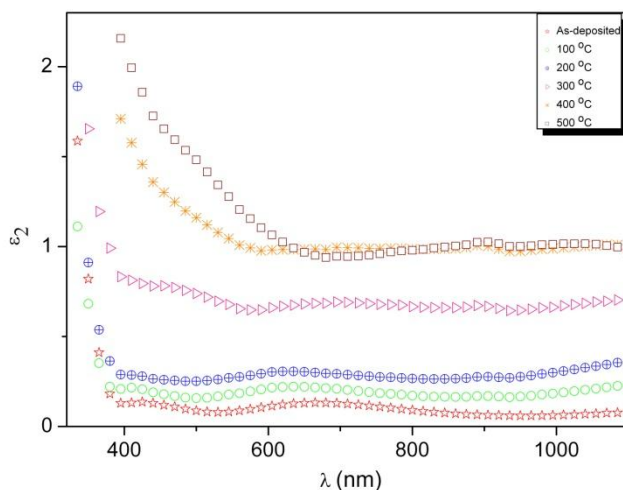
$$\varepsilon_1 = n^2 - k^2 \qquad (7)$$

$$\varepsilon_2 = 2nk \qquad (8)$$

Figure 8 and Figure 9 show the change in the real and imaginary part of the dielectric constant of the film as a function of wavelength, respectively. As seen in both Figures, the actual part of the dielectric constant was higher than that of the imaginary part. Depending on the annealing temperature the real dielectric constant increased from 3.07 to 16.67 while the imaginary part of the dielectric constant increased from 0.08 to 1.24 with at λ=550 nm.

Figure 8. The variation of the real part of the dielectric constant (ε_1) with wavelength as a function of annealed in air at 100-500 $^{\circ}$C.

Figure 9. The variation of the imaginary part of the dielectric constant (ε_2) with wavelength as a function of annealed in air at 100-500 $^{\circ}$C.

4. CONCLUSIONS

In conclusion, the results of the study are summarized as follows:

(i) Mn_3O_4 thin film was grown on the glass substrates by chemical bath deposition method and it formed in tetragonal structure in polycrystalline phase. (ii) XRD measurement showed that the film consists of a stable structure and there is no any phase transitions depending on the annealing temperature. (iii) The film exhibited p-type conductivity, electrical conductivity and mobility were measured as $(1.32-6.65) \times 10^{-6}$ $(\Omega cm)^{-1}$ and 19 to 732 $cm^2(Vs)^{-1}$, respectively as a function of annealing temperature. (iv) The optical transmittance and the energy band gap of the film at room temperature decreased with increasing annealing temperature. (v) Depending on the annealing temperature, extinction coefficient (k) and refractive index (n) increased, k was calculated within the range of 0.024-0.154 and n was calculated within the range of 1.79-3.84.

References

1. L. W. Guo, H. J. Ko, H. Makino, Y. F. Chen, K. Inaba, T. Yao, *J. Cryst. Growth,* 205 (1999) 531-536
2. H. Y. Xu, S. L. Xu, X. Dong Li, H. Wang, H. Yan, *Appl. Surf. Sci.*, 252 (2006) 4091-4096
3. W. Gao, S. Ye, M. Shao, *J. Phys. Chem. Solids,* 72 (2011) 1027-1031
4. S. Sarangapani, B. V. Tilak, C. P. Chen, *J. Electrochem. Soc.,* 143 (1996) 3791-3799
5. M. L. Singla, S. Awasthi, A. Srivastava, *Sensor. Actuat. B,* 127 (2007) 580-585
6. S. K. Park, A. Jin, S. H. Yu, J. Ha, B. Jang, S. Bong, S. Woo, Y. E. Sung, Y. Piao, *Electrochim. Acta,* 120 (2014) 452-459
7. D. P. Dubal, A. D. Jagadale, C. D. Lokhande, *Electrochim. Acta,* 80 (2012) 160-170
8. D. Yang, *J. Power Sources,* 196 (2011) 8843-8840
9. S. Ashoka, G. Nagaraju, G. T. Chandrappa, *Mater. Lett.*, 64 (2010) 2538-2540
10. O. Nilsen, H. Fjellvag, A. Kjekshus, *Thin Solid Films,* 444 (2003) 44-51
11. L. W. Guo, D. L. Peng, H. Makino, K. Inaba, H. J. Ko, K. Sumiyama, T. Yao, *J. Magn. Mater.,* 213 (2000) 321-325
12. L. W. Guo, H. Makino, H. J. Ko, Y. F. Chen, T. Hanada, D. L. Peng, K. Inaba, T. Yao, *J. Crystal. Growth,* 227–228 (2001) 955-959
13. G. M. Jacob, I. Zhitomirsky, *Appl. Surf. Sci.*, 254 (2008) 6671-6676
14. O. Y. Gorbenko, I. E. Graboy, V. A. Amelichev, A. A. Bosak, A. R. Kaul, B. Guttler, V. L.Svetchnikov, H. W. Zandbergen, *Solid State Commun.,* 124, (2002) 15-20
15. J. C. Southard, G. E. Moore, *J. Am. Chem. Soc.*, 64 (1942) 1769-1770
16. A. Gil, L. M. Gandia, S. A. Korili, *Appl. Catal. A,* 274 (2004) 229-235
17. S. Pisdadian, A. M. Shariati Ghaleno, *Acta. Phys. Pol. A,* 123 (4) (2013) 741-745
18. S. Isber, E. Majdalini, M. Tabbal, T. Chiristidis, K. Zahraman, B. Nsouli, *Thin Solid Films,* 517 (2009) 1592-1595
19. A. U. Ubale, M. R. Belkhedkar, Y. S. Sakhare, A. Singh, C. Gurada, D. C. Kothari,*Mater. Chem. Phys.,* 136 (2012) 1067-1072
20. D. P. Dubal, D. S. Dhawale, R. R. Salunkhe, V. J. Fulari, C. D. Lokhande, *J. Alloy. Compd.,* 497 (2010) 166-170
21. H. Dhaouadi, O. Ghodbane, F. Hosni, F. Touati, *ISRN Spectroscopy,* doi: 10.5402/2012/706398.
22. S. Fritsch, J. Sarrias, A. Rousset, G. U. Kulkarni, *Mater. Res. Bull.,* 33 (1998) 1185-1194
23. S. S. Falahatgar, F. E. Ghodsi, F. Z. Tepehan, G. G. Tepehan, İ. Turhan, *Appl. Surf. Sci.,* 289 (2014) 289-299
24. K. J. Kim, Y. R. Park, *J. Crystal. Growth,* 270 (2004) 162-167

25. H. Dhaouadi, A. Madani, F. Touati, *Mater. Lett.,* 64 (2010) 2395-2398
26. C. Ulutas, E. Guneri, F. Kirmizigul, G. Altindemir, F. Gode, C. Gumus, *Mater. Chem.Phys.,* 138 (2013) 817-822
27. C. Gumus, O. M. Ozkendir, H. Kavak, Y. Ufuktepe, *J. Optoelectron. Adv. Mater.,* 8 (1) (2006) 299-303
28. C. Gumus, C. Ulutas, Y. Ufuktepe, *Opt. Mater.,* 29 (2007) 1183-1187
29. M. R. Belkhedkar, A. U. Ubale, *J. Mol. Struct.,* 1068 (2014) 94-100
30. N. M. Hosny, A. Dahshan, Mater. *Chem. Phys.,* 137 (2012) 637-643
31. R. N. Bhargava, D. Gallgher, X. Hong, A. Nurmikko, *Phys. Rev. Lett.,* 72 (1994) 416-419
32. F. Gode, C. Gumus, *J. Optoelectron. Adv. Mater.,* 11 (2009) 429-436
33. A. O. Er, A. H. Farha, C. Gumus, E. Guneri, Y. Ufuktepe, *J. Optoelectron. Adv. Mater.-Rapid Commun.,* 5 (12) (2011) 1286-1291
34. A. M. M. Farea, S. Kumar, K. M. Batoo, A. Yousef, C. G. Lee, Alimuddin, *J. Alloy.   Compd.,* 464 (1-2) (2008) 361-369
35. F. Gode, C. Gumus, M. Zor, *J. Optoelectron. Adv. Mater.,* 9 (7) (2007) 2186-2191